Int. J. Heat Mass Transfer. Vol. 29, No. 6, pp. 879–887, 1986
Printed in Great Britain

0017–9310/86 $3.00 + 0.00
Pergamon Journals Ltd.

Conjugate unsteady heat transfer from a spherical droplet at low Reynolds numbers

DOUGLAS L. R. OLIVER* and JACOB N. CHUNG†

* Mechanical Engineering Department, The University of Toledo, Toledo, OH 43606, U.S.A.
† Mechanical Engineering Department, Washington State University, Pullman, WA 99164, U.S.A.

(*Received* 30 *January* 1985 *and in final form* 17 *December* 1985)

Abstract—The phenomena of conjugate unsteady heat transfer from a spherical droplet or particle moving in a continuous fluid medium is numerically investigated. The energy equation is solved for a spherical droplet using the implicit, finite-difference method of alternating directions (ADI). In this study, the volumetric heat capacities of the two phases are of comparable magnitude but not necessarily equal to each other and the value of the thermal diffusivities of the two phases are set equal to each other. The range of Péclet numbers investigated are: $50 \leqslant Pe \leqslant 1000$, with ratios of volumetric heat capacities, (interior to exterior) varying between 0.333 and 3.0. The velocities used in the convective terms are those corresponding to low Reynolds number flow. It was found that the dimensionless temperature profile asymptotically approaches a steady-state value that is independent of the initial profile in the droplet.

INTRODUCTION

IN MANY situations involving heat transfer from an isolated sphere to an infinite medium, the ratio of thermal properties is such that transfer to only one phase needs to be calculated to obtain a reasonable approximation of the transfer rates. There are two such extreme cases: the so-called, 'external' and 'internal' problems. Both of these special cases postulate an isothermal, interfacial boundary condition, with thermal resistance assumed to be in one phase only.

An example of the external problem (where the resistance is primarily in the continuous phase), is a rain droplet descending in the atmosphere. For a water drop in air, the ratio of volumetric heat capacities H ($H = \rho_1 c_1/\rho_2 c_2$), is about 4000 to 1, with the ratio of thermal conductivities K ($K = H\alpha_1/\alpha_2$), being about 20 to 1. The subscripts 1 and 2 denote the droplet and the continuous phase, respectively. Due to the large value of K and H, this situation may be reasonably modeled as an isothermal sphere with the heat transfer rate governed only by the continuous phase resistance.

Several authors have investigated the special case of the external problem, where the volumetric heat capacity ratio was assumed infinite (thus the sphere remains at its initial temperature). Brunn [1] analytically developed equations for the steady-state Nusselt number at small and large Péclet numbers at low Reynolds numbers for both fluid and solid spheres. Abramzon and Fishbein [2] numerically solved the steady-state energy equation for the case of the external problem with moderate Péclet numbers (up to $Pe = 1000$). Their results suggest that the boundary-layer assumptions are not reasonable for $Pe < 1000$.

The assumption that the temperature of the sphere remains constant is only valid for large ratios of H, where the volumetric heat capacity of the sphere is much larger than that of the continuous phase. If the volumetric heat capacity of the sphere is finite, the temperature of the sphere will eventually approach the ambient temperature. Abramzon and Elata [3] computed the transient heat transfer rates from an isothermal sphere with various finite values of H. They found that for small values of H, the asymptotic Nusselt number would be less than that predicted for a constant temperature sphere. They also found that under certain circumstances local Nusselt numbers, in the aft region of the sphere could be negative, indicating a local reverse flow of energy.

Considering the other extreme case, the internal problem (where the bulk of the resistance is assumed to be in the dispersed phase), there is no equivalent steady-state situation corresponding to the steady-state solution for a constant temperature sphere and therefore a transient solution for the energy equation is sought. For low Péclet numbers, Newman [4] in 1931 presented a solution for diffusion of mass into a sphere. From Newman's work one may show that the Nusselt number (based on the internal properties) asymptotically approaches 6.58. For moderate Péclet numbers, Johns and Beckmann [5] numerically integrated the energy equation for the droplet region. They reported oscillations in the Nusselt number that were due to the recirculation of the fluid inside the droplet. Similar results were obtained using a promising adaptive grid scheme described in Dwyer *et al.* [6]. For high Péclet numbers, a conventional boundary-layer analysis is not appropriate for the internal problem except at very small times, due to the recirculation of fluid inside the droplet. Kronig and Brink [7] analytically solved the energy equation for high Péclet numbers, with the assumption that the isotherms are parallel to the streamlines. As time increases the Nusselt number predicted by the Kronig and Brink model asymptotically approaches a value (based on internal properties) of 17.9.

NOMENCLATURE

a	radius of the sphere
A	ratio of thermal diffusivities, α_1/α_2
c	specific heat
Fo	Fourier number, $\alpha_2 t/a^2$
H	ratio of volumetric heat capacities, $\rho_1 c_1/\rho_2 c_2$
k	thermal conductivity
K	ratio of thermal conductivities, k_1/k_2
Pe	Péclet number, $2aU_\infty/\alpha_2$
Q	net rate of heat diffusing from the sphere
r	dimensionless radial coordinate, R/a
R	radial coordinate
t	time
T	temperature
u	dimensionless radial velocity, U/U_∞
U_∞	velocity of the sphere
v	dimensionless tangential velocity, V/U_∞
W	Zr
X	ratio of dynamic viscosities, μ_1/μ_2
Z	dimensionless temperature, $(T-T_\infty)/(T_{1,0}-T_\infty)$.

Greek symbols

α	thermal diffusivity
Υ	Z/Z_b
ρ	density
η	$1/r$
θ	tangential coordinate.

Subscripts

1	dispersed phase
2	continuous phase
asy	asymptotic
b	bulk
int	interior
ext	exterior
0	initial
∞	free stream.

A third type of transfer from a sphere (the 'conjugate problem'), involves calculation of the temperature field in both the continuous and dispersed phases. As with the internal problem, a transient solution is sought with boundary-layer analyses being inapplicable except at short times. Unlike the internal and external problems, with their constant-temperature interfacial boundaries, continuity of the heat flux is used for the interfacial boundary condition.

For the case of low Péclet number conjugate heat transfer, Cooper [8] developed an analytical solution for the temperature field for various combinations of thermal properties. From Cooper's work one may show that for all conjugate problems, the Nusselt number vanishes for large times with $Pe = 0$, whereas for both the external problem (with $H = \infty$), and the internal problem, the Nusselt numbers asymptotically approach 2.0 and 6.58, respectively.

For high Péclet numbers Chao [9] used boundary-layer assumptions to estimate the heat transfer rates from spheres. Due to the elliptic nature of the interior region, such boundary-layer solutions will be inaccurate except at small times.

Abramzon and Borde [10] used a finite-difference (ADI) method to integrate the energy equation for $0 \leqslant Pe \leqslant 1000$. Both fluid and solid spheres were investigated. This work provides a good literature review and insight into the transport process in droplets and solid spheres. However, Abramzon and Borde's work suffers from two shortcomings: only systems with identical thermal properties in both phases were investigated; and only low Reynolds number flows were considered.

In this study, the work of Abramzon and Borde is expanded by extending their analysis to include fluids with variable ratios of volumetric heat capacities. Since many liquid–liquid systems have Prandtl numbers greater than 100, it is a useful exercise to investigate the transient conjugate heat transfer from droplets translating at low Reynolds numbers, but with moderate Péclet numbers. Due to the many possible permutations in this study, it is limited to systems in which the ratio of thermal diffusivities is one. This limitation is reasonable for certain liquid–liquid hydrocarbon systems since the thermal diffusivity of many liquid hydrocarbons is about $0.9 \times 10^{-7}\ m^2\ s^{-1}$.

MATHEMATICAL MODEL

A spherical droplet of radius a is moving steadily in a continuous medium. The two fluids are immiscible and non-reacting, with no surface active agents. Initially the continuous phase experiences a step temperature change. The properties of the two phases are assumed to be constant and independent of temperature, hence the flow field may be calculated prior to the integration of the energy equation. The flow field is assumed fully developed with the dimensionless velocity profiles being obtained from the creeping flow solution of Hadamard–Rybczinski, thus any effects of surface tension are neglected (see Fig. 1 for a schematic of the system for a fluid droplet):

$$\Psi_1 = \frac{r^4 - r^2}{4(1+X)} \sin^2\theta \tag{1a}$$

$$\Psi_2 = \left[0.5r^2 - \frac{2+3X}{4(1+X)} r + \frac{1}{4(1+X)r}\right] \sin^2\theta \tag{1b}$$

$$u_1 = \frac{r^2-1}{2(1+X)} \cos\theta, \quad v_1 = \frac{1-2r^2}{2(1+X)} \sin\theta \tag{2a}$$

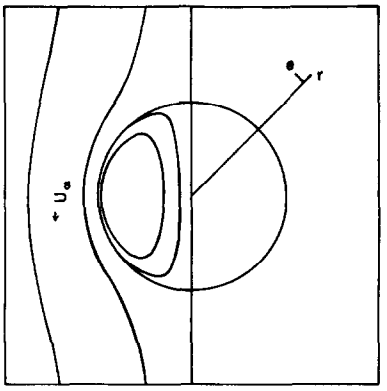

FIG. 1. Schematic of the coordinate system and the flow lines for a fluid sphere.

$$u_2 = \left[1 - \frac{2+3X}{2(1+X)r} + \frac{X}{2(1+X)r^3}\right]\cos\theta$$
$$v_2 = \left[-1 + \frac{2+3X}{4(1+X)r} + \frac{X}{4(1+X)r^3}\right]\sin\theta. \quad (2b)$$

The uncoupled dimensionless energy equation may be shown to be:

$$\frac{\alpha_2}{\alpha_j}\frac{\partial Z}{\partial Fo_2} + \frac{\alpha_2}{\alpha_j}\frac{Pe_2}{2}\left[u\frac{\partial Z}{\partial r} + \frac{v}{r}\frac{\partial Z}{\partial\theta}\right] = \frac{\partial^2 Z}{\partial r^2} + \frac{2}{r}\frac{\partial Z}{\partial r} + \frac{1}{r^2}\cot\theta\frac{\partial Z}{\partial\theta} + \frac{1}{r^2}\frac{\partial^2 Z}{\partial\theta^2} \quad (3)$$

where Z is the dimensionless temperature based on the initial temperature difference:

$$Z = (T - T_\infty)/(T_{1,0} - T_\infty). \quad (4)$$

The dimensionless parameters: Fo (Fourier number), given by $Fo = \alpha_2 t/a^2$ and Pe (Péclet number), $Pe = 2aU_\infty/\alpha_2$, are based on the external properties. The initial and boundary conditions are:

Initial conditions

$$Z(r, \theta, t = 0) = 1, \quad 0 < r < 1 \quad (5)$$
$$Z(r, \theta, t = 0) = 0, \quad 1 < r < \infty. \quad (6)$$

Boundary conditions

$$K\frac{\partial Z_1}{\partial r} = \frac{\partial Z_2}{\partial r}, \quad \text{at} \quad r = 1$$
(continuity of heat flux) (7a)
$$Z_1 = Z_2 \quad \text{at} \quad r = 1 \quad (7b)$$
$$Z(r, \theta, t) = 0, \quad r \to \infty \quad (8)$$
$$\frac{\partial Z}{\partial\theta} = 0, \quad \text{for} \quad \theta = 0 \quad \text{and} \quad \theta = \pi$$
also, Z is finite at $r = 0$. (9)

SOLUTION PROCEDURE

At the droplet center ($r = 0$) the boundary condition on $Z(r = 0)$ is imposed by defining a new variable for the interior region: $W = Zr$. Thus the boundary condition at the droplet center becomes:

$$W(r = 0, t) = 0. \quad (10)$$

With the transformed energy equation for the droplet phase being:

$$A^{-1}\frac{\partial W}{\partial Fo_2} + \frac{Pe_2}{2A}\left[u\left(\frac{\partial W}{\partial r} - \frac{W}{r}\right) + \frac{v}{r}\frac{\partial W}{\partial\theta}\right] = \frac{\partial^2 W}{\partial r^2} + \frac{1}{r^2}\cot\theta\frac{\partial W}{\partial\theta} + \frac{1}{r^2}\frac{\partial^2 W}{\partial\theta^2}. \quad (11)$$

In the exterior region, a high density of nodes are used near the interface, with fewer nodes near the free stream. This is accomplished by using the transformation $\eta = 1/r$. This transformation appears to be a better choice than the usual transformation $\xi = \ln(r)$, in that the former transformation allows one to obtain a close spacing near the interface, without regard to the exact location at which the free-stream conditions are imposed, since $\eta = 0$ is a 'point at infinity'. The transformation $\eta = 1/r$ also needs fewer total nodal points for comparable grid spacing at the interface. The transformed energy equation for the continuous phase is given by:

$$\frac{\partial Z}{\partial Fo_2} + \frac{Pe_2}{2}\left[-\eta^2 u\frac{\partial Z}{\partial\eta} + \eta v\frac{\partial Z}{\partial\theta}\right] = \eta^4\frac{\partial^2 Z}{\partial\eta^2} + \eta^2\cot\theta\frac{\partial Z}{\partial\theta} + \eta^2\frac{\partial^2 Z}{\partial\theta^2}. \quad (12)$$

The initial conditions for interior and exterior points are:

$$W(r, \theta, t = 0) = r, \quad 0 < r < 1 \quad (13)$$
$$Z(\eta, \theta, t = 0) = 0, \quad 0 < \eta < 1. \quad (14)$$

The boundary conditions imposed on equations (11) and (12) are:

$$W(r = 0, t) = 0, \quad (15)$$
$$K\left(\frac{\partial W}{\partial r} - \frac{W}{r}\right) + \frac{\partial Z}{\partial\eta} = 0, \quad \text{at} \quad r = 1, \quad \eta = 1 \quad (16a)$$
$$W = Z \quad \text{at} \quad r = 1, \quad \eta = 1 \quad (16b)$$
$$\frac{\partial W}{\partial\theta} = 0, \quad \frac{\partial Z}{\partial\theta} = 0, \quad \text{for} \quad \theta = 0 \quad \text{and} \quad \theta = \pi \quad (17)$$
$$Z(\eta = 0, \theta, t) = 0 \quad \text{(free-stream condition)}. \quad (18)$$

Equations (11) and (12) were solved with a ADI procedure similar to that used by Abramzon and Borde [10], the primary exceptions being the transformation used in equation (12), and the interfacial boundary condition [equation (16a)]. It was not found necessary to use any up-wind differencing scheme to model the convective terms, these terms were modeled with central-difference approximations. Equations (11) and

(12) yield the following discrete approximations:

$$\frac{1}{A}\frac{dW_{i,j}}{dFo_2}+\left(\frac{Pe\,u}{4A\Delta r}-\frac{1}{\Delta r^2}\right)W_{i+1,j}+\left(\frac{-Pe\,u}{4A\Delta r}-\frac{1}{\Delta r^2}\right)W_{i-1,j}+\left(\frac{Pe\,v}{4Ar\Delta\theta}-\frac{\cot\theta}{2r^2\Delta\theta}-\frac{1}{r^2\Delta\theta^2}\right)W_{i,j+1}+\left(\frac{-Pe\,v}{4Ar\Delta\theta}+\frac{\cot\theta}{2r^2\Delta\theta}-\frac{1}{r^2\Delta\theta^2}\right)W_{i,j-1}+\left(\frac{-Pe\,u}{2Ar}+\frac{2}{\Delta r^2}+\frac{2}{r^2\Delta\theta^2}\right)W_{i,j}=0 \quad (19)$$

$$\frac{dZ_{i,j}}{dFo_2}+\left(\frac{Pe\,u\eta^2}{4\Delta\eta}-\frac{\eta^4}{\Delta\eta^2}\right)Z_{i+1,j}+\left(\frac{-Pe\,u\eta^2}{4\Delta\eta}-\frac{\eta^4}{\Delta\eta^2}\right)Z_{i-1,j}+\left(\frac{Pe\,v\eta}{4\Delta\theta}-\frac{\eta^2\cot\theta}{2\Delta\theta}-\frac{\eta^2}{\Delta\theta^2}\right)Z_{i,j+1}+\left(\frac{-Pe\,v\eta}{4\Delta\theta}+\frac{\eta^2\cot\theta}{2\Delta\theta}-\frac{\eta^2}{\Delta\theta^2}\right)Z_{i,j-1}+2\left(\frac{\eta^4}{\Delta\eta^2}+\frac{\eta^2}{\Delta\theta^2}\right)Z_{i,j}=0. \quad (20)$$

The step size $\Delta\eta$ is chosen such that $\Delta\eta=\Delta r/(\Delta r+1)$.

With this step size and the initial conditions at the interface, a control volume analysis yields the initial interfacial temperature of:

$$W(r=1,\theta,t=0)=Z(\eta=1,\theta,0)=H/[(1+\Delta r)+H]. \quad (21)$$

The interfacial boundary condition [equation (16a)] is approximated by:

$$\frac{K\Delta\eta}{\Delta r}(W_{m-2,j}-4W_{m-1,j})+\left(\frac{3K\Delta\eta}{\Delta r}-2K\Delta\eta+3\right)W_{m,j}-4Z_{m+1,j}+Z_{m+2,j}=0 \quad (22)$$

where m denotes the column corresponding to the interfacial boundary.

The symmetrical boundaries [equation (17)] are modeled as:

$$W_{i,3}-4W_{i,2}+3W_{i,1}=0 \quad (23a)$$

$$W_{i,m-2}-4W_{i,m-1}+3W_{i,m}=0, \quad \text{for all } i. \quad (23b)$$

[Note: Z replaces W in equations (23a) and (23b) for $r>1$, and m denotes the final tangential column.]

When equations (19) and (20) are treated in the normal ADI method, a tridiagonal matrix results everywhere except at the interfacial boundary [equation (22)], and at the symmetrical boundaries [equations (23a) and (23b)]. At these three boundaries the tridiagonal algorithm is modified to account for the additional matrix components which are outside the main three bands. A 41×41 grid was used for $Pe<1000$ (i.e. $\Delta r=1/40, \Delta\theta=\pi/40$), a 51×51 grid was used for $Pe=1000$. The time step used varied with each simulation, depending on the Péclet number, the ratio of thermal diffusivities, and the ratio of viscosities. For each simulation the time step was held constant. The time step was not increased with time for two reasons: the system might be unstable if time step was too large, and the LU decompositions of the resulting matrices needed to be recomputed with each change in the time step size. Further details of the solution procedure and the grid dependence are given in Oliver [13].

COMPARISONS WITH PREVIOUS INVESTIGATIONS

The above model and coding may be verified and benchmarked against the results of several previous investigators. The Nusselt number will be used to compare the present model with the various special cases cited above. The bulk dimensionless temperature is given as:

$$Z_b=\frac{3}{2}\int_0^\pi\int_0^1 Zr^2\sin\theta\,dr\,d\theta. \quad (24)$$

The Nusselt number is defined by the relation:

$$Nu_2=\frac{2aQ}{4\pi a^2(T_{1,b}-T_\infty)K_2} \quad (25)$$

which is equivalent to:

$$Nu=\frac{-2}{3}H\frac{1}{Z_b}\frac{dZ_b}{dFo}. \quad (26)$$

One may also calculate the Nusselt number by calculating the flux of heat from the surface of the sphere:

$$Nu=\frac{1}{Z_b}\int_0^\pi\left.\frac{\partial Z_2}{\partial\eta}\right|_{\eta=1}\sin\theta\,d\theta. \quad (27)$$

If H is large, or if the time steps are small, then the change in the bulk temperature with each time step might be small. Under these conditions equation (26) will not be a good predictor of the Nusselt number since the bulk temperature changes slowly. Even with $H=1$, there may be a significant difference in the Nusselt number predicted by equations (26) and (27), particularly at large Péclet numbers (i.e. for large times, about 2–3% for $Pe\simeq500$, $A=1$, and $H=1$ with a 41×41 grid mesh). This difference may be reduced by increasing the number of nodes used. Generally, equation (27) was used to calculate the Nusselt numbers.

For the case of low Péclet number heat transfer, the predictions of the present model may be compared with the analytic solution of Cooper [8]. From the work of Cooper, an explicit equation for both the Nusselt

number and the bulk temperature may be shown to be:

$$Z_b = 6/\pi K A^{1/2} \int_0^\infty [G(u)/u^2]\,du \tag{28}$$

$$Nu = 2/3K \frac{\int_0^\infty G(u)\,du}{\int_0^\infty G(u)u^{-2}\,du} \tag{29}$$

where

$$G(u) = \frac{\exp(-u^2 AFo)(u\cos u - \sin u)^2}{\{Au^2 \sin^2 u + [K(u\cos u - \sin u) + \sin u]^2\}}.$$

Equations (28) and (29) were numerically integrated using Gauss quadrature methods for several values of H and A. In Fig. 2, the Nusselt numbers based on the analytical work of Cooper are plotted for comparison with the values predicted by the present numerical model. For all cases tested, it was found that there is a good agreement between equation (29) and the present model (with $Pe = 0$), except for extreme cases such as very short times, or extreme ratios of thermal properties.

The present model has also been tested against the numerical solution of Johns and Beckmann [5] for the special case of the internal problem. For comparison with the internal problem, both the Nusselt number and the Fourier number reported in their work (which are based on internal properties) must be converted to parameters which are based on the external properties. The internal problem has been approximated by setting the volumetric heat capacity ratio to $H = 0.005$ with the ratio of diffusivities set to $A = 2$. Simulations were performed for $Pe = 320$ and 640 with a ratio of viscosities of $X = 0$. In Fig. 3 the Nusselt numbers predicted by the present model as compared with the appropriate cases reported by Johns and Beckmann are plotted.

For the case of external resistance, the present model (with $H = 100$, $A = 1$) has been compared with the transient solution for the external problem presented in Abramzon and Elata [3] (with $H = \infty$) for $Pe = 300$ and $Pe = 1000$. The Nusselt number predicted by the present model is plotted in Fig. 4 for comparison with the results reported by Abramzon and Elata.

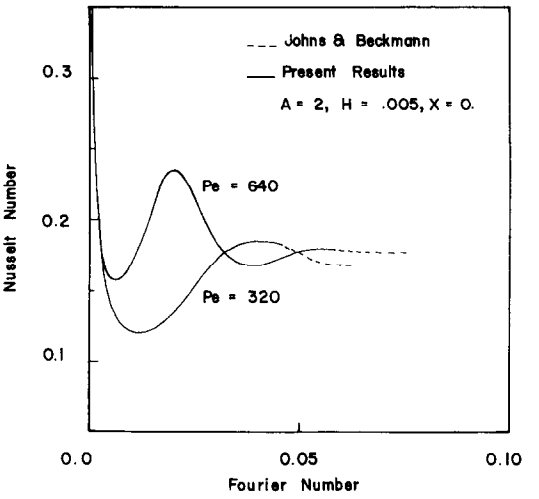

FIG. 3. Nusselt number for the interior problem; comparison with the solution of Johns and Beckmann.

In all cases tested—the low Péclet number conjugate problem, the internal problem, and the external problem—the present model compares favorably with the special cases cited above.

RESULTS AND DISCUSSION

Initially the sharp gradients near the interface cause a rapid rate of heat transfer with a correspondingly high Nusselt number. For a fluid sphere at moderate Péclet numbers the Nusselt number oscillates with a decaying amplitude. The oscillations are due to the circulation of the fluid, in the interior of the droplet. This circulation of fluid alternately supplies hot and cold fluid to the fore region of the droplet where most of the transfer takes place. As time increases the Nusselt number asymptotically approaches a steady value. The Nusselt

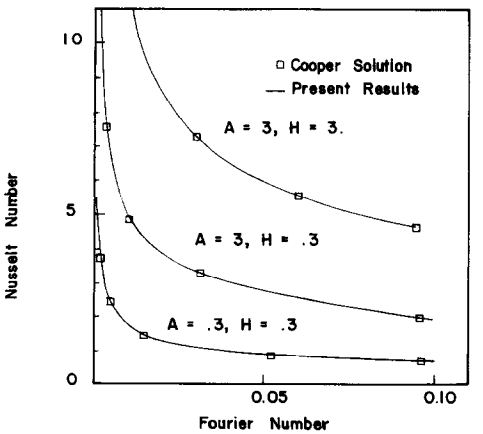

FIG. 2. Nusselt number for $Pe = 0$; comparison with the solution of Cooper.

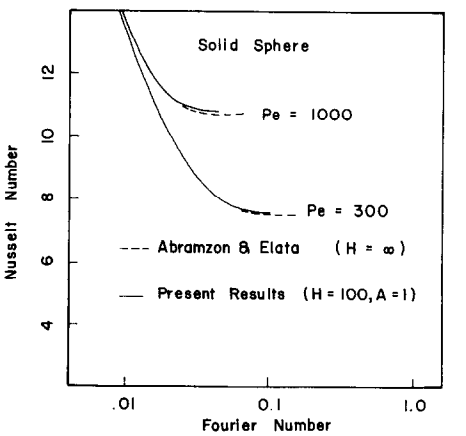

FIG. 4. Nusselt number for the external problem; comparison with the solution of Abramzon and Elata.

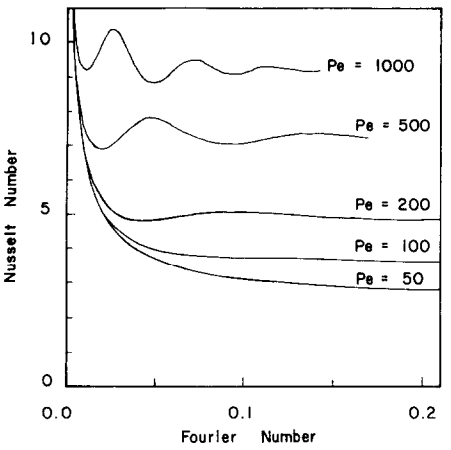

FIG. 5a. Nusselt numbers for a droplet with $X = 1$ and $H = 1$, $A = 1$.

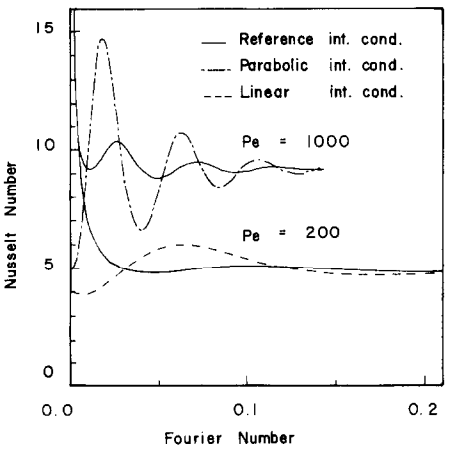

FIG. 6a. Nusselt number as a function of the initial temperature inside the droplet with $X = 1$, $H = 1$ and $A = 1$.

number for a solid sphere also approaches an asymptotic value, but without any oscillations. Such behavior of the Nusselt number is illustrated in Figs. 5a and b.

The asymptotic Nusselt number appears to be a good parameter for quantifying the transfer capabilities of a particular system. It appears to be independent of both time and of the initial temperature profile of the sphere, whereas the initial transient behavior of the Nusselt number is a strong function of the initial conditions in the sphere. As an example of this independence, several simulations were made with initial conditions that were other than those given in equation (5). Specifically, cases were simulated using parabolic and linear initial temperature profiles:

$$Z(r, \theta, 0) = 1 - r^2 \text{ (parabolic)}, \quad 0 < r < 1$$

and

$$Z(r, \theta, 0) = 1 - r \text{ (linear)}, \quad 0 < r < 1.$$

The simulations with the parabolic initial conditions were made with $H = 1$ and $Pe = 1000$ for both a fluid sphere and a solid sphere. Similar calculations were made with the linear initial profile for $H = 1$ and $Pe = 200$. The Nusselt numbers predicted for these four simulations are shown in Figs. 6a and b for comparison with the Nusselt numbers predicted with the reference initial conditions [equation (5)]. Note the dependence (at small times) of the Nusselt number on the initial conditions and the independence of the asymptotic behavior of the Nusselt number on the initial temperature profile of the sphere.

The primary frequency of oscillation of the Nusselt number, for a fluid sphere, is also independent of the initial temperature profile of the sphere. This demonstrates that the oscillations in the Nusselt number are due to the circulation of fluid inside the droplet, which is independent of the initial temperature profiles.

Since the value of the asymptotic Nusselt number appears to be independent of the initial conditions of the sphere, it is an important parameter with respect to comparing heat transfer capabilities of various systems. Abramzon and Borde [10] proposed the simple predictive equation for the asymptotic Nusselt number:

$$Nu_{asy} \simeq \left[\frac{1}{K\,Nu_{int}} + \frac{1}{Nu_{ext}}\right]^{-1} \tag{30}$$

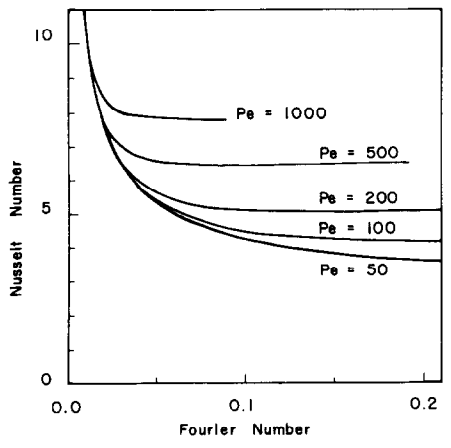

FIG. 5b. Nusselt number for a solid sphere with $H = 3$, $A = 1$.

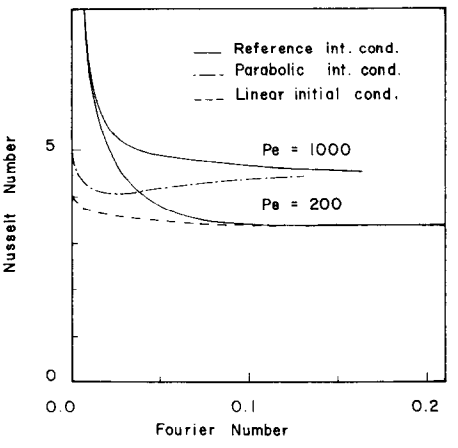

FIG. 6b. Nusselt number as a function of the initial temperature inside a solid sphere with $H = 1$ and $A = 1$.

with Nu_{int} representing the asymptotic value of the Nusselt number for the interior problem (based on the properties of the droplet phase), and Nu_{ext} representing the asymptotic value of the Nusselt number for the exterior problem with $H = \infty$. The values of the asymptotic Nusselt numbers for the interior problem may be read from a graph on p. 60 of Clift *et al.* [11]. The values of the asymptotic Nusselt numbers for the exterior problem may be read from a chart presented in Abramzon and Fishbein [2].

Abramzon and Borde showed that equation (30) predicted Nu_{asy} reasonably well for moderate Péclet numbers for the special case of H other than 1. To test the accuracy of equation (30) for other moderate values of H, the values of the asymptotic Nusselt number predicted by the present finite-difference model are listed in Table 1, with the values of the asymptotic Nusselt number predicted by equation (30) listed in parenthesis. A note of caution should be made regarding the asymptotic Nusselt number; the decay to a steady value of the Nusselt number was often slow, especially for low Péclet numbers. Thus it was difficult to determine the exact asymptotic value of the Nusselt number, particularly for low Péclet numbers. A small time step was required since instabilities were noticed with this solution procedure. Thus, computer time limitations prevented the use of a strict convergence criterion.

Equation (30) adequately predicts the asymptotic value of the Nusselt number for moderate Péclet numbers. At low Péclet numbers equation (30) will overpredict the asymptotic Nusselt number. For pure diffusion, the interior problem and the exterior problem both have finite values for the asymptotic Nusselt number (6.6 and 2.0, respectively), thus equation (30) would predict a finite value for the asymptotic Nusselt number for the conjugate problem for $Pe = 0$. However, from the analytic work of Cooper [8] it may be shown that the asymptotic Nusselt number for the conjugate problem with pure diffusion ($Pe = 0$) is zero. Thus equation (30) will overpredict the asymptotic Nusselt number at low Péclet numbers for conjugate problems.

The asymptotic value of the Nusselt number is the result of the asymptotic behavior of the dimensionless temperature profiles when scaled by the dimensionless bulk temperature. Define: $\Upsilon(r, \theta)$ to be the local dimensionless temperature scaled by the dimensionless temporal bulk temperature, i.e. $\Upsilon(r, \theta, t) = Z(r, \theta, t)/Z_b$. As time increases Υ becomes independent of both time and the initial temperature profile of the sphere. The independence of Υ on both time and the initial conditions is illustrated well by Figs. 7a and b. In these figures, the contours of Υ are plotted for two cases. Each has a different initial temperature profile and a different bulk temperature, and each temperature profile is evaluated at different times yet they both have essentially identical contour profiles of Υ.

The steady-state profiles of Υ for $Pe = 100$ and $Pe = 1000$ have been plotted on Figs. 8 and 9. The same viscosity ratio and thermal conductivity ratios were used so that the development of the temperature profiles with respect to the Péclet number could be observed in Figs. 7–9. At lower values of Péclet numbers, where conduction is still quite important,

Table 1. (a) Approximate asymptotic value of the Nusselt number: solid spheres, $A = 1$

Pe	Interior* problem	$H = 0.333$	$H = 1$	$H = 3.0$	Exterior† problem ($H = \infty$)
50	6.6	1.15(1.39)	2.24(2.74)	3.4(3.8)	4.7
100	6.6	1.46(1.46)	2.82(3.0)	4.2(4.4)	5.6
200	6.6	1.67(1.53)	3.4(3.3)	5.1(5.1)	6.8
500	6.6	1.86(1.61)	4.1(3.8)	6.5(6.1)	8.9
1000	6.6	1.94(1.67)	4.6(4.1)	7.9(7.0)	10.9

(b) Approximate asymptotic value of the Nusselt number: fluid spheres, $X = 1$, $A = 1$

Pe	Interior‡ problem	$H = 0.333$	$H = 1$	$H = 3.0$	Exterior† problem
50	8.2	1.40(1.70)	2.67(3.3)	4.0(4.5)	5.5
100	11.2	2.03(2.26)	3.6(4.3)	5.2(5.8)	6.9
200	14.9	2.67(2.98)	4.8(5.6)	6.9(7.5)	9.0
500	17.1	4.0(3.7)	7.2(7.4)	10.2(10.4)	13.1
1000	17.7	4.6(4.1)	9.2(8.8)	13.5(13.2)	17.6

* Newman.

† Obtained by solving numerically the energy equation for the external region.

‡ Obtained by solving the energy equation for the interior problem. The Nusselt number in this case is based on the internal properties (Nu_1).

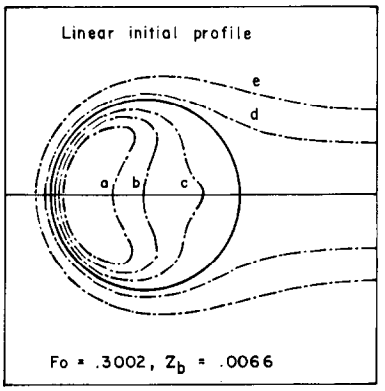

a : Υ = 1.4, b : Υ = 1.1, c : Υ = 0.8, d : Υ = 0.3, e : Υ = 0.1

FIG. 7a. Profile of Υ for a fluid sphere with a linear initial temperature profile inside the sphere with $Pe = 200$, $X = 1$ and $H = 0.333$.

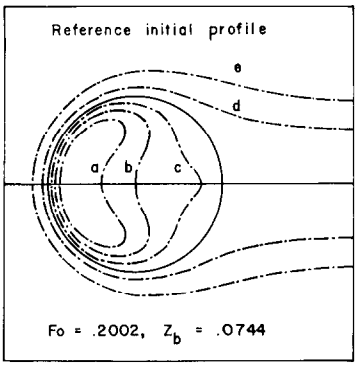

a : Υ = 1.4, b : Υ = 1.1, c : Υ = 0.8, d : Υ = 0.3, e : Υ = 0.1

FIG. 7b. Profile of Υ for a fluid sphere with the reference initial profile [equation (5)], with $Pe = 200$, $X = 1$ and $H = 0.333$.

there is little correlation between the temperature contours and the streamline contours. For larger values of Péclet numbers, the temperature contours begin to resemble the streamline contours, except near the upstream region of the continuous phase.

Finally, the above result may be readily applied to the problem of mass transfer to droplets and particles.

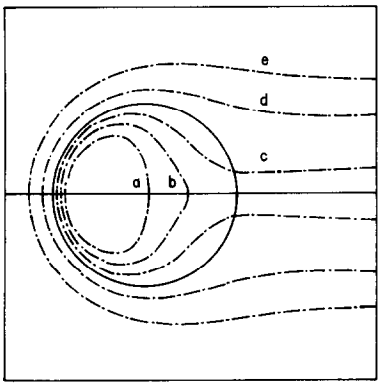

a : Υ = 1.4, b : Υ = 1.1, c : Υ = 0.8, d : Υ = 0.3, e : Υ = 0.1

FIG. 8. Asymptotic profile for Υ for a droplet with $X = 1$, $H = 0.333$ and $Pe = 100$.

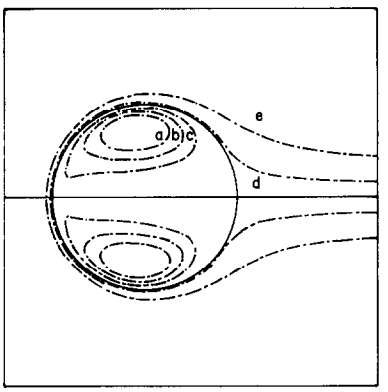

a : Υ = 1.4, b : Υ = 1.1, c : Υ = 0.8, d : Υ = 0.3, e : Υ = 0.1

FIG. 9. Asymptotic profile for Υ for a droplet with $X = 1$, $H = 0.333$, $Pe = 1000$.

Clift *et al.* [11] present a good review of the one to one correspondence of heat and mass transfer in droplets under certain circumstances.

CONCLUSION

The unsteady conjugate heat transfer rates from a fluid sphere and a spherical particle have been numerically estimated for low Reynolds number flows, where the thermal diffusivities of the two phases are equal, with ratios of the thermal capacities of $0.333 \leqslant H \leqslant 3$, and for Péclet numbers of $50 \leqslant Pe \leqslant 1000$.

The temperature profile, when made dimensionless by the difference between the temporal bulk temperature of the sphere and the ambient temperature, appears to decay to an asymptotic steady-state profile that is independent of both time and the initial conditions of the droplet. As a result of this asymptotic behavior of the dimensionless temperature profile, the Nusselt number also asymptotically approaches a steady-state value. The value of the asymptotic Nusselt number may be adequately approximated, for the range of parameters investigated, by the relation given in equation (30).

Acknowledgements—This work was initiated while the first author was supported by a fellowship funded by the U.S. D.O.E. while at Washington State University. The graphics were made by Rochana Junkasem.

REFERENCES

1. P. O. Brunn, Heat or mass transfer from single spheres in a low Reynolds number flow, *Int. J. Engng Sci.* **20,** 817–822 (1982).
2. B. M. Abramzon and G. A. Fishbein, Some problems of convective diffusion to a spherical particle with $Pe \leqslant 1000$, *J. Engng Phys.* **32,** 682–686 (1977).
3. B. M. Abramson and C. Elata, Unsteady heat transfer from a single sphere in Stokes flow, *Int. J. Heat Mass Transfer* **27,** 687–695 (1984).
4. A. B. Newman, The drying of porous solids : diffusion and

surface emission equations, *Trans. Am. Inst. chem. Engrs* **27**, 203–211 (1931).
5. L. E. Johns, Jr. and R. B. Beckmann, Mechanism of dispersed-phase mass transfer in viscous, single-drop extraction systems, *A.I.Ch.E. Jl* **12**, 10–16 (1966).
6. H. A. Dwyer, R. J. Kee and B. R. Sanders, Adaptive grid method for problems in fluid mechanics and heat transfer, *AIAA Jl* **18**, 1205–1212 (1980).
7. R. Kronig and J. C. Brink, On the theory of extraction from falling droplets, *Appl. Sci. Res.* **A2**, 142–155 (1950).
8. F. Cooper, Heat transfer from a sphere to an infinite medium, *Int. J. Heat Mass Transfer* **20**, 991–993 (1976).
9. B. T. Chao, Transient heat and mass transfer to a translating drop, *Trans. Am. Soc. mech. Engrs*, Series C, *J. Heat Transfer* **91**, 273–281 (1969).
10. B. M. Abramzon and I. Borde, Conjugate unsteady heat transfer from a droplet in creeping flow, *A.I.Ch.E. Jl*, **26**, 536–544 (1980).
11. R. Clift, J. R. Grace and M. E. Weber, *Bubbles, Drops and Particles*. Academic Press, New York (1978).
12. G. Dahlquist, A. Bjork and N. Anderson, *Numerical Methods*. Prentice-Hall, Englewood Cliffs, NJ (1974).
13. D. L. R. Oliver, Ph.D. Thesis, Washington State University, Pullman, WA (1985).

TRANSFERT THERMIQUE CONJUGUE, VARIABLE D'UNE GOUTTE SPHERIQUE A FAIBLE NOMBRE DE REYNOLDS

Résumé—On étudie les phénomènes de transfert thermique conjugué variable à partir d'une goutte ou d'une particule se déplaçant dans un milieu continu fluide. L'équation d'énergie est résolue pour une sphérule par une méthode implicite de différences finies avec directions alternées (ADI). Dans cette étude, les capacités thermiques volumiques des deux phases sont comparables mais pas nécessairement égales et les valeurs des diffusivités thermiques des deux phases sont égales. Le domaine des nombres de Péclet sont $50 < Pe < 1000$, avec des rapports des capacités thermiques volumiques (intérieure à extérieure) variant entre 0,333 et 3,0. Les vitesses utilisées dans les termes convectifs sont ceux correspondant à l'écoulement à faible nombre de Reynolds. On trouve que le profil de température adimensionnel approche asymptotiquement une valeur permanente qui est indépendante du profil initial dans la goutte.

GEKOPPELTE INSTATIONÄRE WÄRMEÜBERTRAGUNG VON EINEM KUGELFÖRMIGEN TROPFEN BEI NIEDEREN REYNOLDSZAHLEN

Zusammenfassung—Das Phänomen der gekoppelten instationären Wärmeübertragung von einem kugelförmigen Tröpfchen oder Partikel, das sich in einem Fluid bewegt, wird numerisch untersucht. Die Energiegleichung wird für einen kugelförmigen Tropfen mit dem impliziten Differenzenverfahren für alternierende Richtungen (ADI) gelöst. Bei dieser Untersuchung sind die volumetrischen Wärmekapazitäten der beiden Phasen von vergleichbarer, aber nicht notwendigerweise gleicher Größe. Der Wert der Temperaturleitfähigkeit der beiden Phasen wird als gleich angenommen. Der Bereich der untersuchten Peclet-Zahlen erstreckt sich von $50 < Pe < 1000$; dabei variieren die Verhältnisse der volumetrischen Wärmekapazitäten (innere zu äußere) von 0,333 bis 3,0. Die in den Termen für Konvektion benützten Geschwindigkeiten entsprechen Strömungen mit niederer Reynolds-Zahl. Es ergab sich, daß das dimensionslose Temperaturprofil sich dem Wert eines stationären Zustandes, der vom anfänglichen Profil im Tropfen unabhängig ist, annähert.

СОПРЯЖЕННЫЙ НЕСТАЦИОНАРНЫЙ ТЕПЛОПЕРЕНОС СФЕРИЧЕСКОЙ КАПЛИ ПРИ МАЛЫХ ЧИСЛАХ РЕЙНОЛЬДСА

Аннотация—Численно исследуется сопряженный нестационарный теплообмен движущейся сферической капли или частицы со сплошной жидкой средой. Уравнение энергии для сферической капли решается неявным конечно-разностным методом переменных направлений. Объемные теплоемкости обеих фаз сравнимы между собой, но не обязательно равны, а их температуропроводности считаются одинаковыми. Исследования проводятся в диапазоне чисел Пекле от 50 до 1000, причем отношения объемных теплопроводностей (внутренней и наружной фаз) изменяются от 0,333 до 3,0. Скорости, используемые в конвективных членах, соответствуют течению при малых числах Рейнольдса. Найдено, что профиль безразмерной температуры асимптотически приближается к стационарному профилю, независимому от его начальной конфигурации в капле.